Multi-Objective Optimization and Experimental Investigation of Quarter Car Suspension System

Abstract: The primary function of the suspension system is to improve ride comfort and vehicle control. However, typical passive suspension systems have to do this contradicting task. In order to do this task, one needs to tune/optimize the suspension parameters. This study presents a methodology for determining the optimal suspension settings for a quarter-car suspension system. Macpherson strut suspension is used to construct a test rig and simulate a quarter-car suspension system. For ride comfort and optimization purpose, a Macpherson strut model is implemented in Matlab/Simulink® environment. The suspension system is optimized for ride comfort and stability. Frequency weighted RMS acceleration, vibration dose value (VDV), Maximum transient vibration value (MTVV) objectives are used for ride comfort and for stability RMS suspension deflection and RMS tire deflection are used as objective function during optimization study. As a result, the optimization problem becomes multi objective type, and the spring stiffness and suspension damping are optimized using the NSGA-II algorithm. Further, the optimized strut is installed and tested on quarter car test rig and further, on car to validate the results. The simulation results and test rig results are obtained and validated. From test rig and vehicle results, optimized strut improves ride comfort, by reducing RMS acceleration, VDV and MTVV and provides vehicle stability. The study of optimized strut on vehicle is conducted using four road surfaces and four different drivers. The findings are represented graphically in time as well as frequency domain and also in tabular form.

Keywords: Multi-Objective Optimization, NSGA-II, Ride Comfort, Quarter Car Test Rig, Macpherson Strut.

1. Introduction

An automobile comprises of various systems and subsystems. One such system is the suspension system, which has the tasks of supporting the vehicle's weight, aiding in its maneuverability, and isolating the occupants from road irregularities to provide a comfortable ride. However, for the conventional suspension system, also known as a passive suspension system, this task is a conflicting one. As stiff suspension system is required to support the weight and follow the track whereas the soft suspension system is required to provide ride comfort. Hence a passive suspension system has to simultaneously perform these conflicting requirements. Thus, a suspension system needs to be optimized to perform main objectives such as to provide ride comfort, road handling, and suspension travel [1].

For modelling and optimization purposes, Guo and Zhang [2] have modelled suspension systems such as a quarter vehicle model with 2 degrees of freedom, a half car model with 4 degrees of freedom, and a full automobile model with 7 degrees of freedom. Using Hamming and Runge-Kutta techniques, simulation results were obtained. Using the NSGA-II method, a multi-objective optimization problem was constructed for vehicle models with ISO class road surfaces. Authors had suggested the use of DoE method along with optimization algorithms to avoid local minima or maxima solutions. Optimized parameters showed better results over conventional suspension parameters.

Zadeh and et al. [3] studied a 5 DoF half car model, including 1 DoF human model. The vehicle model was moving over a double bump type road surface with a velocity of 20 m/s. The multi-objective study consists of 5 objectives, which include seat acceleration, suspension deflection of both suspensions and velocities of both tires. Out of these 5 objectives, different pairs of objectives were formed to form a bi-objective optimization problem. The results were presented in the time domain. It was observed that 5 objective optimization results were superior to that of 2-objective optimization.

Optimization of quarter car model with linear spring was presented by Alkhatib and et al. [1]. Authors had described a bi-objective optimization problem consisting of RMS acceleration and RMS suspension space objectives and solved by implementing a genetic algorithm. The authors had suggested adding a mechanical filter to isolate sprung mass, leading to a 3 DoF system.

Shojaeefard and et al. [4] had implemented a half car model having 4 DoF along with single DoF lumped mass human model for optimization study using NSGA-II algorithm. Four different Pareto-fronts were identified and analyzed by the authors. The trade-off points were obtained by TOPSIS method. On the basis of performance, it is observed that an optimized suspension system gives better outcomes.

The optimization of a light commercial vehicle was performed by Ozcan et al. [5]. A quarter car and a half car model were used to assess and enhance the vehicle's ride and handling characteristics. The RMS body acceleration, body roll, and tire forces were the performance criterions under consideration. The models were modelled and simulated in Matlab/Simulink, and the resulting findings were evaluated for optimization analysis. From an initial optimization run based on data provided by car manufacturers, the curve fitting methodology was used to optimize suspension parameters. Authors have implemented Carmaker® model to validate the performance of the optimized suspension unit.

Genetic algorithm (GA), sequential quadratic program (SQP), and pattern search algorithm (PSA) algorithms were used by Zhangzhe and et al. [6] for optimization study. A linear quarter car suspension system is optimized for suspension acceleration, working space, and tire forces as design objectives. GA and PSA were more reliable optimization methods as compared to the SQP. The performance assessment was carried out on the results based on a random road and various vehicle speeds. It was observed that optimization improves the design criterion.

A coupled 3-DoF drive-quarter car model had optimized by Kuznetsov and et al. [7] where driver is modelled as 1-DoF and 2-DoF vehicle. A global optimization problems (AGOP) algorithm was implemented for optimization and ride comfort was assessed using ISO 2631-1 standard. Three types of road surfaces from Australia were selected for further analysis. All three types of road surfaces were analyzed based on ISO-2631 health risk criterion. Influence of tire stiffness, suspension stiffness, and suspension damping was analyzed, and it was observed that the damping coefficient significantly influenced riding comfort.

GA based optimization of 4-DoF driver-car system, comprising of vehicle driver model having 2-DoF each, was presented by Gundogdu [8]. Acceleration of head, crest factor, suspension deflection and tire deflection were the objective function involved in the study. The author had used non-dimensional expressions and converted the objective functions into uni-objective function. While doing so, each objective function was assigned with equal weight. The genetic algorithm was implemented to search the optimal suspension and seat parameters. It was observed that the solutions were having lower values of overshoot and settling time yields minimum VDV and CF.

It observed that, from [1-6], author have studied spring stiffness and suspension damping as the most critical factors during optimization for ride comfort and vehicle handling. Moreover, quarter car with driver model have also implemented by authors [7-8] to study ride comfort and optimization.

Patil and Joshi [9] developed a simple 2 DoF quarter car suspension system for active control applications. A rigid frame supports sprung, and unsprung masses was constrained to move vertically using a vertical guide bar. The unsprung mass was excited by a cam and follower mechanism through the DC motor. The active

suspension system comprising of a hydraulic actuator for vibration control. It was concluded that the active system improved ride performance compared to the passive system. Salah [10] had designed a test bench to study the behavior of quarter car with various road conditions. The test bench consists of a rigid frame on which sprung mass, and unsprung mass was mounted as rigid plates. The vertical motion of these masses was achieved through vertical bars. A mechanism was used to simulate bump and hump inputs to the systems. A hydraulic cylinder actuator was used for active control applications. Sensors are mounted on the test rig to record the data through LabVIEW software. The test rig is useful for laboratory teaching, training, and research purposes.
Koch and et al. [11] had developed quad vehicle a quarter car test platform. Firstly, a passive system was developed and tested, and then the same was further modified for active suspension control. The test platform consists of two masses, sprung and unsprung, comprising of a solid steel plate and tire and suspension elements respectively. The tire was excited by a linear motor which emulates road surface. The sprung mass was free to move vertically along linear guides. Accelerometers and force sensors were used to record the data. Ahmandian and Pare [12] studied semi-active suspension control using a quarter car test setup. The test rig was excited by a hydraulic actuator. A MR damper was used to study various semi-active suspension configurations viz. sky hook, ground hook, and hybrid control. Series of experiments were performed, and it was observed that ground hook control provide better road holding and improves stability compared to the passive system. Skyhook control reduces sprung mass transmissibility considerably. Additionally, the hybrid control strategy, a mix of combination of sky- and ground hook, provided better ride and stability.
Sandu et al. [13] studied a quarter car test rig comprising of Macpherson strut suspensions. A non-linear model was developed as the equations of motions consist of angles. The author had used a 2004 Porche 996 car's suspension attached to the test rig. The test bench composed of fixed frame, sprung and unsprung mass. Linear guides were used to observe the vertical moment of the sprung mass. The tire was actuated by a servo-hydraulic actuator. Sensors were mounted on key locations to record the data. The experimental data proved that the nonlinear multi-body model was developed accurately and can be further used for controller design.
Various suspension test rigs, from simple laboratory setup to advanced Macpherson strut system, were developed by [9-13] for ride applications.
In this study a 2-DoF quarter car suspension system and test setup developed using a Macpherson strut. The suspension system is modelled in MATLBA/Simulink® environment for ride comfort and optimization study. The suspension system is optimized using multi-objective NSGA-II algorithm considering
The test setup is developed using suspension configuration of an Indian small car Nano. The quarter car suspension system is modelled using a Macpherson strut, in MATLAB/Simulink® environment. The suspension parameters are then optimized for ride comfort and road holding using NSGA-II algorithm. The optimized parameters are then implemented on quarter car test rig and actual car model.

2. Materials and Methods

2.1. Modelling of Macpherson Strut Suspension System

To study the dynamic behavior of suspension system and to optimize the suspension parameters to satisfy desired objective functions a mathematical model is required which is based on functional requirements. In this study a Macpherson strut model is used hence the model is developed in MATLAB/Simulink® environment for ride comfort and optimization study. Earl Macpherson has developed the Macpherson strut suspension model for Ford in the year 1994. The Macpherson strut suspension system has found its application in variety of vehicles due to light weight and simple in construction.
This study employs a mathematical model of the Macpherson strut suspension model developed by Hong et al [14]. The schematics of the Macpherson strut is depicted in Figure 1. Let us consider the Macpherson suspension system is excited by road unevenness (x_r), as represented in Figure 1. The suspension system consists of a quarter portion of a car body, a tire, spindle, control arm, and a strut. The model has 2 DoFs - sprung mass vertical displacement, and rotational motion of the control arm. This model assumes bushing pin joint at O and neglect strut mass. Equation 1 represents a 2-DoF Macpherson suspension model.
Equation of Motion for Macpherson Strut Model [14] is -

$$\left.\begin{array}{l}(m_s + m_{us})\ddot{x}_s + m_{us} l_c \cos(\theta - \theta_0)\,\ddot{\theta} - m_{us} l_c \sin(\theta - \theta_0)\,\dot{\theta}^2 + k_t(x_s + l_c(\sin(\theta - \theta_0) - \sin(-\theta_0) - x_r)) = 0 \\ m_{us} l_c^2 \ddot{\theta} + m_{us} l_c \cos(\theta - \theta_0)\,\ddot{x}_s + \frac{c_p b_1^2 \sin(\alpha' - \theta_0)\dot{\theta}}{4(a_1 - b_1 \cos(\alpha' - \theta))} + k_t l_c \cos(-\theta_0)\,(x_s l_c \sin(\theta - \theta_0) - \sin(-\theta_0)) - x_r - \\ \frac{1}{2} k_s \sin(\alpha' - \theta)\left[b_1 + \frac{d_1}{(c_1 - d_1 \cos\,(\alpha' - \theta)^{\frac{1}{2}})}\right] = 0\end{array}\right\} \quad (1)$$

Where,
$\alpha' = \alpha + \theta_0$, $a_1 = l_A^2 + l_B^2$, $b_1 = 2 l_A l_B$, $c_1 = a_1^2 - a_1 b_1 \cos(\alpha - \theta_0)$, $d_1 = a_1 b_1 - b_1^2 \cos(\alpha - \theta_0)$

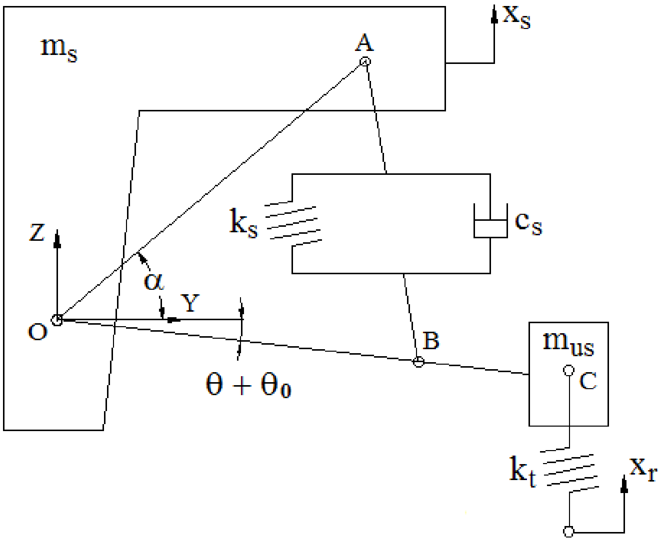

Figure 1. Quarter car model with Macpherson strut [14].

2.2 Quarter Car Test Setup

A quarter car test setup is developed using Macpherson strut suspension. The test setup consists of a quarter portion of the vehicle. The setup is 2-DoF quarter car model with vertical plate of sprung mass and strut, lower control arm, tie rod, and tire with rim constituting unsprung mass. Two vertical guide shafts coupled to a vertical plate (representing sprung mass) and support frame with linear bearings to move plate vertically. The system is pneumatically excited through cylinders and Selec® controller. The Selec® controller controls the ON/OFF timings of the DC valve, which in turn excites the pneumatic cylinder. Table 1 represents the ON/OFF timings of the controller. The setup performance, i.e. sprung and unsprung mass acceleration, is recorded using a Class 1 SVAN 958A sound and vibration analyzer. Figure 2 represents a Macpherson strut test setup whereas Figure 3 depicts accelerometer mounting on the setup.

Table 1. Controller ON/OFF Timings Scenario.

Scenario No.	On Time (ms)	Off Time(ms)
S1	13	12
S2	12	8
S3	9	7
S4	8	6
S5	6	4

Figure 2. Setup of Quarter Car Test Rig.

(**a**) (**b**)

Figure 3. Position of Accelerometers: (**a**) Sprung mass; (**b**) Unsprung mass

2.3 Multi-Objective Optimization (MOO) of Quarter Car Suspesnion System

In this study a multi-objective optimization problem is formed and simulated in MATLAB/Simulink® environment. The responses of suspension system such as frequency weighted RMS acceleration, VDV and MTTV are the significant parameters as ride comfort and health is concerned. Along with these, suspension space and tire deflection are also considered as objective functions for vehicle handling. Thus, these five objectives form a multi-objective optimization problem.

2.3.1. MOO – Problem Formulation

Frequency weighted RMS sprung mass Acceleration: Frequency weighted RMS acceleration, according to ISO 2631-1 [15], is defined as -

$$A_w = \left\{\frac{1}{T}\int_0^T [a_w(t)]^2 dt\right\}^{\frac{1}{2}} \tag{2}$$

A major portion of vibrations, that experiences due to road unevenness, enters the passenger's body through seat [16,17]. The whole-body vibrations (WDV), which affects human body mostly, transmitted via seat along vertical column through buttock and back. It is advised to measure these body vibrations as it directly affects the health risk with increase in vibration exposure time. According to ISO 2631-1, VDV can be used as a measure to access WBV. VDV accesses the cumulative effect or dose of WBV.

Vibration Dose Value (VDV): VDV can be calculated as fourth power of acceleration time histories readings. Here VDV is calculated at sprung mass. VDV is expressed as [15] -

$$\mathrm{VDV} = \left\{\int_0^T [a_w(t)]^4 dt\right\}^{\frac{1}{4}} \tag{3}$$

Maximum Transient Vibration Value (MTVV): During the measuring cycle, MTVV is the highest vibration level [15].

$$\mathrm{MTVV} = \max\,(a_w) \tag{4}$$

Suspension Deflection: It is the relative displacement between the masses namely sprung and unsprung. It is represented by -

$$\text{Suspension Deflection (SD)} = x_s - x_{us} \tag{5}$$

Thus, RMS suspension deflection is proposed as one of the objective functions.

$$\text{RMS SD} = \left\{\frac{1}{T}\int_0^T [(x_s(t) - x_{us}(t))]^2 dt\right\}^{\frac{1}{2}} \tag{6}$$

Dynamic Tire Deflection: Tire deflection is the measure of dynamic tire force and is calculated as follows: -

$$\text{Tire Deflection (TD)} = x_{us} - x_r \tag{7}$$

Another objective function introduced here is RMS tire deflection.

$$\text{RMS TD} = \left\{\frac{1}{T}\int_0^T [(x_{us}(t) - x_r(t))]^2 dt\right\}^{\frac{1}{2}} \tag{8}$$

To avoid hitting suspension stops maximum sprung mass acceleration should not exceed 4.5 m/s^2 whereas suspension space required is 125 mm, at least. Also, to keep dynamic tire forces minimum, tire deflection should not exceed 0.058 m [18]. Thus, these parameters are included in objective function formulation as constraints.

The optimization problem is formulated having 5 objective functions as follows –

f_1 = Minimize (VDV)
f_2 = Minimize (Aw)
f_3 = Minimize (MTVV)
f_4 = Minimize (RMS SD)
f_5 = Minimize (RMS TD)

The constraint to the optimization problem are -

Maximum $a_w \leq 4.5 m/s^2$, Maximum $(SD) \leq 0.125m$, Maximum. $(TD) \leq 0.058$ m,

2.3.2. Search Space

In this optimization problem, stiffness and damping of suspension are the design variable. The search space for design variables is defined as –

For spring stiffness, $k_s \in \pm 50\%\ k_s$, and for damping, $c_s \in \pm 50\%\ c_s$, [8]

Thus, range of suspension spring stiffness, $k_s \in [7675, 23027]$, and for damping $c_s \in [230, 692]$

2.3.3. Population

One of the most significant aspects of GA is determining population size. The range of design variables is deciding factor for population i. e. k_s and c_s.

Hence (23027-7675=) 15352 is the range of k_s. For chromosome to store value of k_s, (2^{13} =) 8192 < 15352<(2^{14})= 16384, 14 bits are needed. Refer Table 2 for analysis of variable c_s.

Table 2. Design Variable Range.

Design Variable	Range	Size	
k_s	23027-7675 = 15352	2^{13} = 8192 < 15352<2^{14} = 16384	14 bits
c_s	692-230 = 462	2^8 = 256 <462<2^9 = 512	09 bits

To hold design variables, overall length of gene is 23 (=14+09) bits, of which 14 bits are used to store k_s, and remaining 09 bits are used to store c_s.
To determine optimum population size Rosenthal and Borschbach [19] concluded that population size 70-100 yields best performance for NSGA-II algorithm. According to Hernandez-Diaz et al. [20] population size of 52 is sufficient to obtain good performance for NSGA-II.
According to Reeves and Rowe [21] principle, starting from initial population, every point must be reachable in search space. GA initiates random population, thus, probability of at least one allele to be present at each locus is expressed by formula [21] -

$$P_2^* = (1-(1/2)^{N-1})^{l_s} \tag{9}$$

Where N = Population size and l_s = string length
Following equation represent population size using exponential function approximation [21] –

$$N \approx [1+\log(-l_s/\ln P_2^*)/\log 2] \tag{10}$$

According to equation (10), to exceed 99.9% probability, for string of 50 length population size of 17 is sufficient.
Alander [22] has suggested the relation for population size -
$l_s \leq N \leq 2l_s$, where l_s is length of the string.
Hence, according to [19-22] population size of 100 is selected for optimization study stopping criterion for algorithm is number of generations. After 100 generations, the algorithm is terminated.

2.3.4. Algorithm Parameters

This study uses NSGA-II [23] algorithm. A NGPM code (NSGA-II Program in MATLAB) is implemented [24, 25] for optimization. NGPM is the implementation of NSGA-II (Non-dominated Sort Genetic Algorithm) in MATLAB. The optimization algorithm parameters implemented are tabulated in Table 3.

Table 3. Optimization Algorithm Parameters –NSGA-II

Algorithm	Population	Mutation Probability	Cross-over probability	Generatio ns	Function Evaluations
NSGA-II	100	1/no. of variables (2)	0.9	100	10000

3. Results and Discussion

The test setup is first deployed with the initial/unoptimized strut. The pneumatic system and DC valve are then used to simulate the setup. The time history data of sprung and sprung mass is acquired and processed using FFT analyzer. Simulated in experimental results are tabulated in Table 4. It has been found that the simulated outcomes and the experimental ones, viz. the measurements, including RMS acceleration, VDV, MTTV, suspension space, and tire deflection, are quite in good agreement. Figure 4 shows comparative bar chart of simulated and experimental results. Figure 5 shows time domain results of simulated and experimental case of scenario S1. The figure shows time histories of sprung mass acceleration, suspension space deflection and tire deflection. Form Figure 5 it is observed that simulated and experimental results are in close agreement.

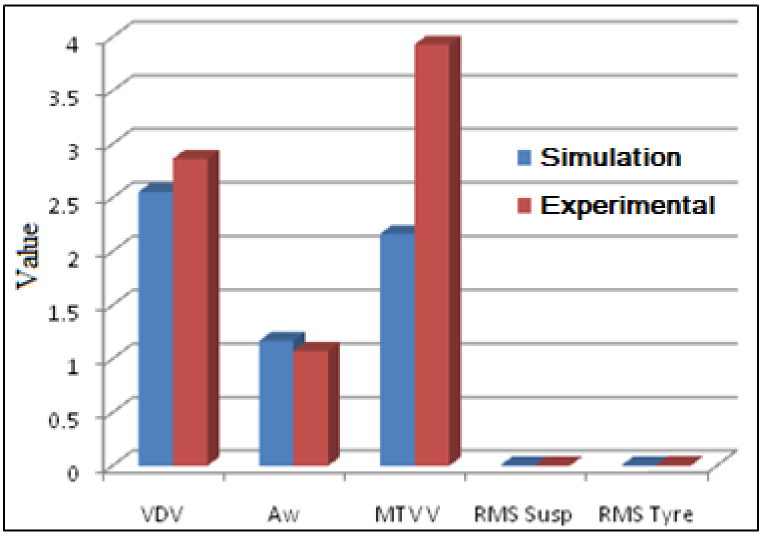

Figure 4. Comparative Analysis – Simulation and Experimental Results (Scenario – S1).

Table 4. Test Setup Results – Simulated (S), Experimental (E).

Parameter	**Scenario – S1**		**Scenario - S2**		**Scenario - S3**		**Scenario - S4**		**Scenario – S5**	
	S	**E**	**S**	**E**	**S**	**E**	**S**	**E**	**S**	**E**
VDV	2.5543	2.8648	4.5065	3.4155	4.3095	3.1118	3.5504	3.2294	3.1649	3.1599
Aw	1.1707	1.0757	1.6796	1.4877	1.9183	1.1590	1.6416	1.4238	1.5282	1.3934
MTVV	2.1649	3.9336	3.7213	5.1305	3.3704	3.4986	4.7663	3.4194	2.8137	2.7534
R-SD	0.0071	0.0062	0.0275	0.0436	0.0250	0.0193	0.0557	0.0395	0.0441	0.0455
R-TD	0.0068	0.0081	0.0226	0.0221	0.0288	0.0186	0.0320	0.0260	0.0223	0.0166
Max A	4.9087	4.3136	8.2320	4.6917	7.5372	4.8060	6.2060	3.9602	4.7397	3.8533
Max SD	0.0139	0.0137	0.0826	0.0578	0.0570	0.0520	0.1355	0.0915	0.0721	0.0935
Max TD	0.0152	0.0163	0.0638	0.0623	0.0627	0.0483	0.0784	0.0630	0.0361	0.0333

R-SD:RMS Suspension Deflection, R-TD: RMS Tire Deflection, Max A: Maximum Acceleration,
Max SS: Maximum Suspension Deflection   Max TD: Maximum Tire Deflection

Frequency response plot of simulated and experimental results of scenario S1 is shown if Figure 6. Figure 6 one can conclude that, for un-optimized strut, the simulated and experimental results are in good agreement.
The un-optimized strut is further simulated on the test setup for scenarios S2, S3, S4, and S5. Time histories of results are obtained and are represented in Table 4 and time domain results are shown in Figure 7 and 8. A good agreement is observed between simulated and experimental results.

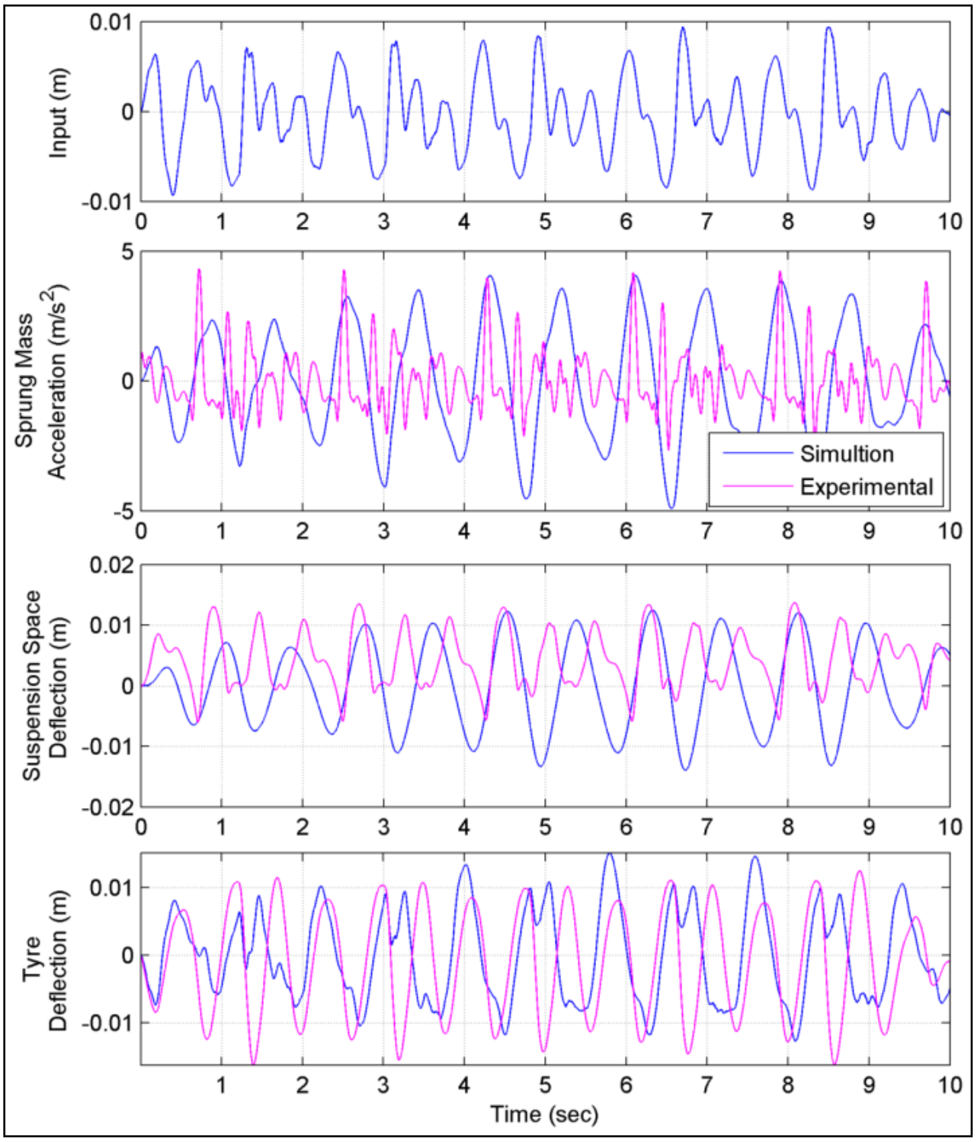

Figure 5. Time Domain Test Setup Results – Simulation and Experimental (Scenario – S1).

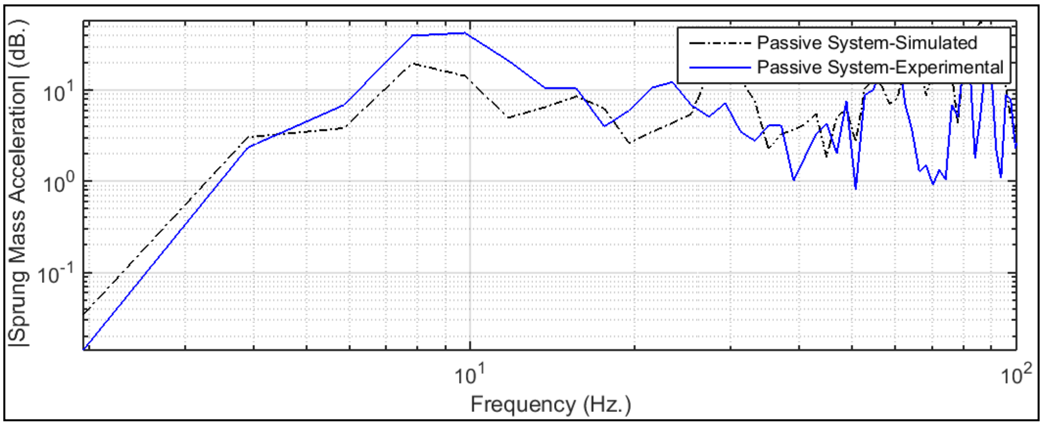

Figure 6: A Frequency Response Plot of Un-optimized Strut - Simulated and Experimental Results

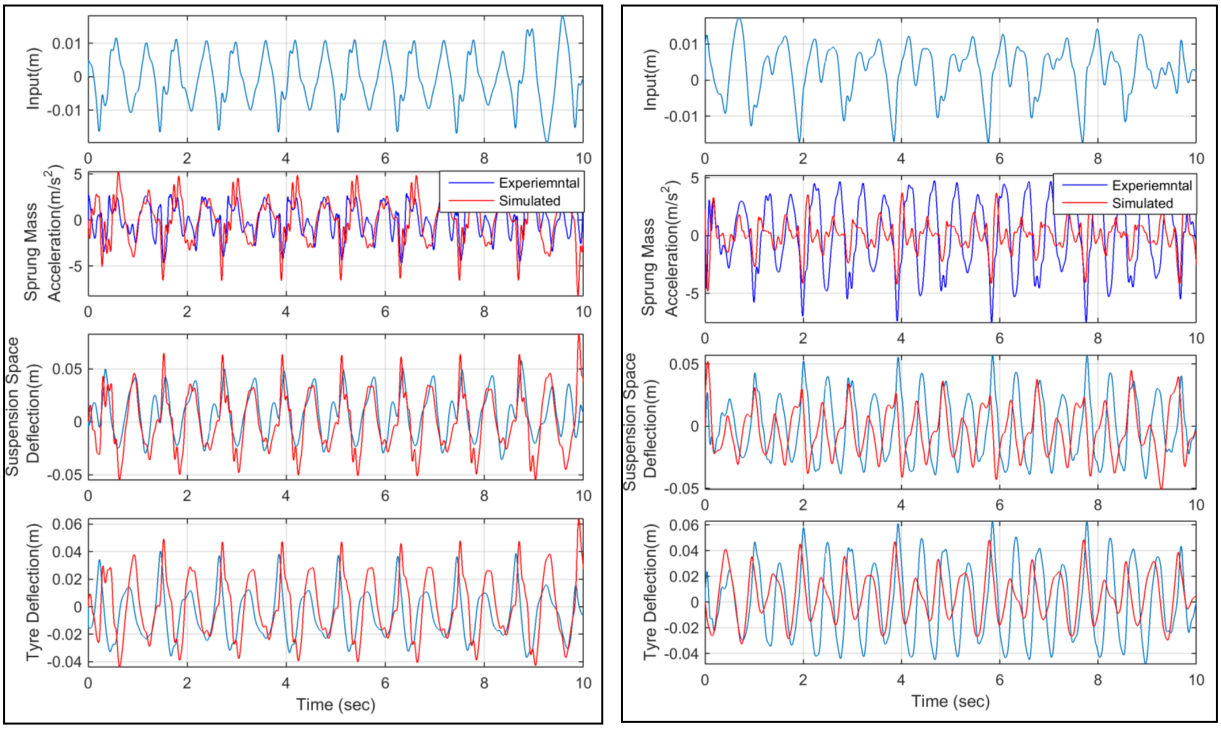

(**a**) (**b**)

Figure 7. Time Domain Results of Test Setup – Simulated and Experimental: (**a**) Scenario – S2; (**b**) Scenario – S3.

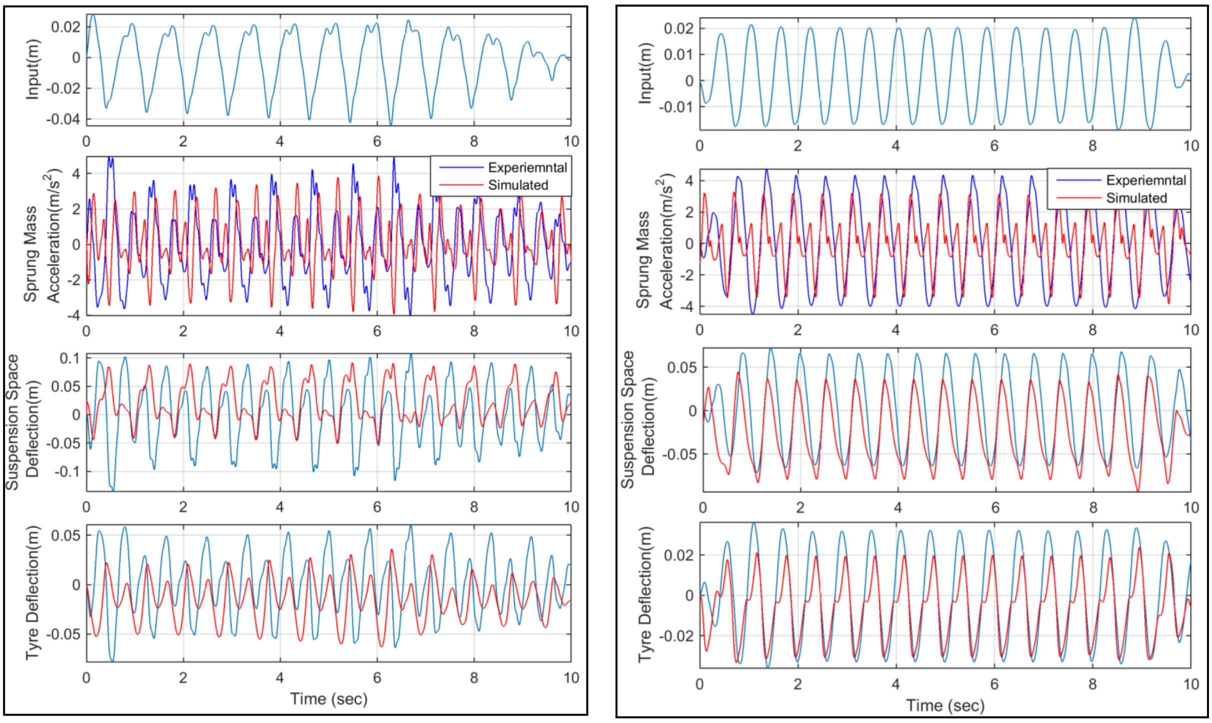

(**a**) (**b**)

Figure 8. Time Domain Results of Test Setup – Simulated and Experimental: (**a**) Scenario – S4; (**b**) Scenario – S5.

From Figure 5 – Figure 8 and Table 4, it is observed that the simulation and experimental results are in good agreement with each other, hence for further analysis mathematical model is used for simulation and optimization of the quarter car test setup. The test setup is further used for experimental validation of optimum suspension parameters.

3.1. Multi-Objective Optimization and Experimental Validation – Test Setup

Optimum suspension parameters are obtained by optimizing the mathematical model using NSGA-II algorithm in MATLAB/Simulink®. As the population size is of 100 genes, hence a trade-off front obtained after optimization has 100 different solutions. All these 100 solutions satisfy the constraints. Figure 8 represents the trade-off front of all 5 objective functions. A solution is chosen from among the 100 solutions that meets the ride and health criteria, which means it has the lowest values of RMS acceleration, VDV, and MTVV. This solution is then simulated further for experimental validation. Table 5 represents optimized strut parameters.

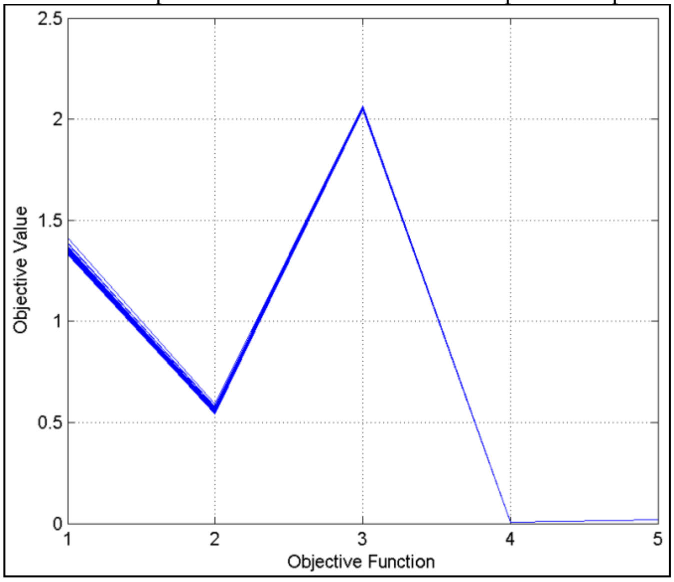

Figure 9. Trade-off front – NSGA-II Optimization.

Table 5. Optimized Suspension Parameters

Parameters	Value
k_s	11509.5131
c_s	318.3712

The test setup is then simulated with strut having optimized suspension parameters. The time histories are obtained. Figure 10 depicts the findings of the time domain data for sprung mass acceleration, suspension space, and tire deflection. In comparison to the un-optimized suspension system, the optimized suspension system has reduced values of sprung mass acceleration, suspension deflection, and tire deflection (see Figure 10). The optimized suspension system has lower values of RMS sprung mass acceleration, VDV, and MTTV. As compared to unoptimized suspension system, optimized suspension parameters have VDV lowered by 45%, RMS acceleration of sprung mass reduced by 47% and MTTV is decreased by 42%. Thus, by minimizing RMS sprung mass acceleration and VDV, the optimized suspension system increased ride comfort and health criteria. The optimized suspension system also provides stability and follows constraints. Refer Table 6 and Figure 11 showing bar chart for comparative results.

Frequency domain results of experimental responses of the optimized and un-optimized strut are shown in Figure 12. In comparison to un-optimized strut, the experimental result demonstrates a less magnitude of sprung mass acceleration for optimized strut parameters, at 10 Hz frequency level.

Table 7 shows % of improvement of optimized suspension parameters over un-optimized parameters. From Table 6 and Table 7, it is observed that the optimized parameter reduces the VDV and RMS acceleration, thus improving the ride and health parameters also providing vehicle stability.

The test is further simulated for scenarios S-2 to S-5, and the results are presented in Figure 13 and Figure 14. Overall improvement in ride and comfort is observed.

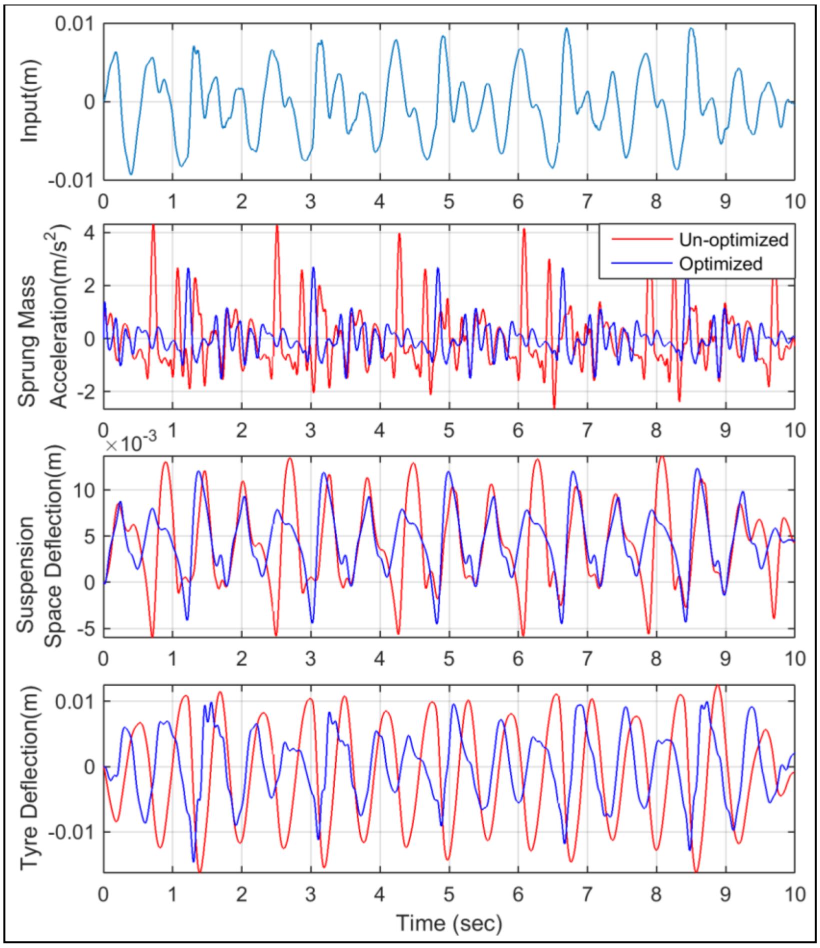

Figure 10. Experimental Time Domain Result (Scenario – S1)

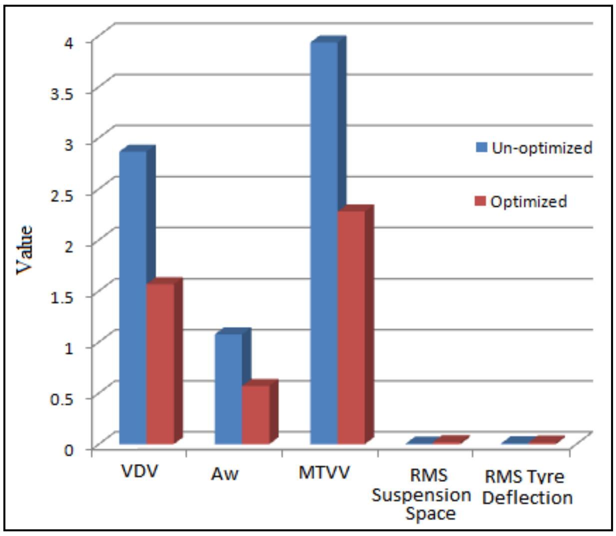

Figure 11. Bar Charts - Analysis of optimized and un-optimized Results for Scenario – S1.

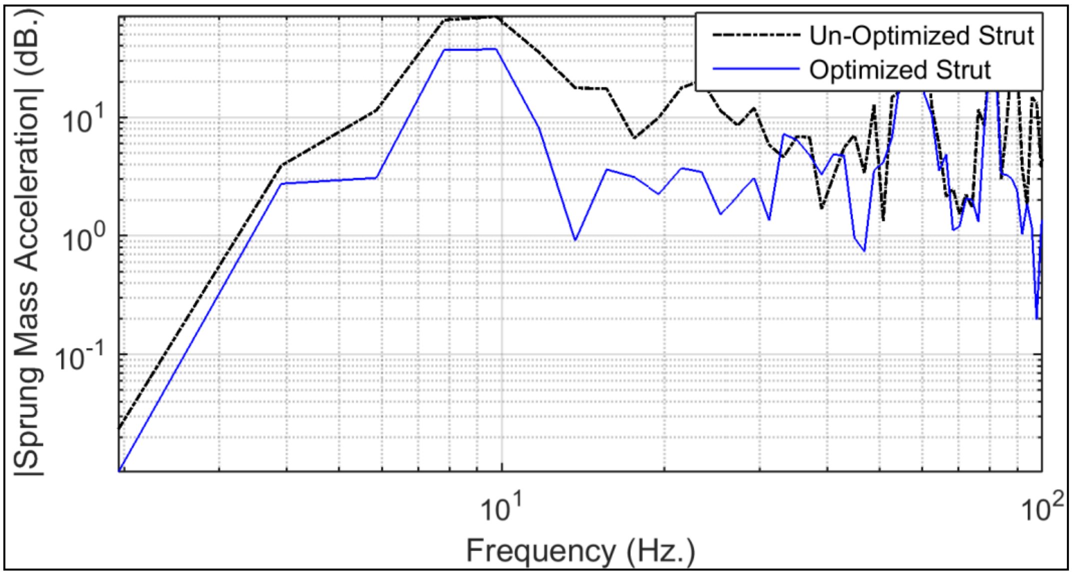

Figure 12. Experimental Results - Frequency Response Plots (Optimized and Un-optimized Strut).

Table 6. Test Setup Results for Un-Optimized (U) and Optimized (O) Strut

Parameter	**Scenario – S1**		**Scenario - S2**		**Scenario - S3**		**Scenario - S4**		**Scenario – S5**	
	U	**O**	**U**	**O**	**U**	**O**	**U**	**O**	**U**	**O**
VDV	2.8648	1.5673	3.4155	1.7826	3.1118	2.7086	3.2294	1.9578	3.1599	1.7716
Aw	1.0757	0.5695	1.4877	0.7786	1.5190	1.1985	1.4238	0.9045	1.3934	0.6411
MTVV	3.9336	2.2782	5.1305	2.9910	3.4986	2.3303	3.4194	2.0060	2.7534	2.6880
R-SD	0.0062	0.0057	0.0436	0.0241	0.0231	0.0227	0.0395	0.0244	0.0455	0.0328
R-TD	0.0081	0.0052	0.0221	0.0073	0.0186	0.0165	0.0260	0.0240	0.0166	0.0158
Max A	4.3163	2.6997	4.6917	2.8584	4.8060	3.9863	3.9602	2.4247	3.8533	3.2997
Max SD	0.0137	0.0124	0.0578	0.0590	0.0520	0.0624	0.0915	0.0537	0.0935	0.0768
Max TD	0.0163	0.0146	0.0623	0.0173	0.0483	0.0343	0.0630	0.0417	0.0333	0.0343

R-SD: RMS Suspension Deflection, R-TD: RMS Tire Deflection, Max A: Maximum Acceleration, Max SD: Maximum Suspension Deflection, Max TD: Maximum Tire Deflection.

Table 7. Percentage Improvement of Optimized Parameters

Parameter	**S1**	**S2**	**S3**	**S4**	**S5**
VDV	45.29	47.80	12.95	39.37	43.93
Aw	47.05	47.66	21.09	36.47	53.99
MTVV	42.08	41.70	33.39	41.33	2.37
RMS Suspension Deflection	8.06	44.72	01.73	38.22	27.91
RMS Tire Deflection	35.80	66.96	11.29	7.69	4.81

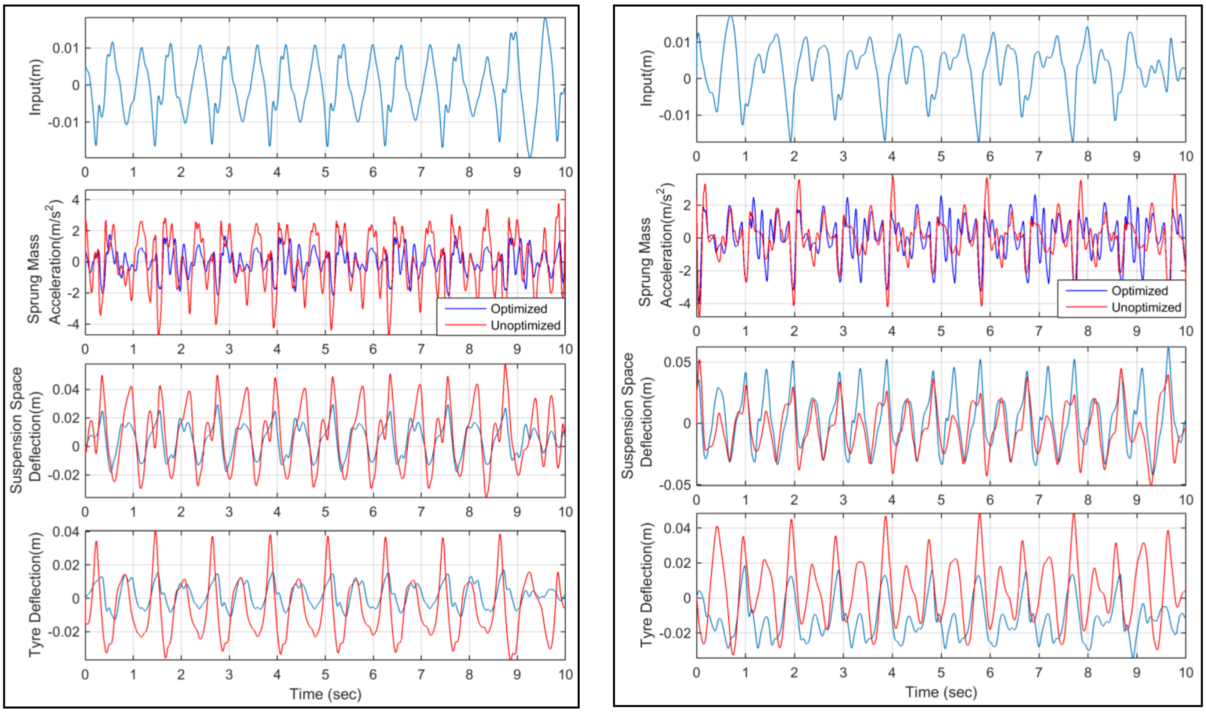

(**a**) (**b**)

Figure 13. Experimental Results – Time Domain: (**a**) Scenario-S2; (**b**) Scenario-S3.

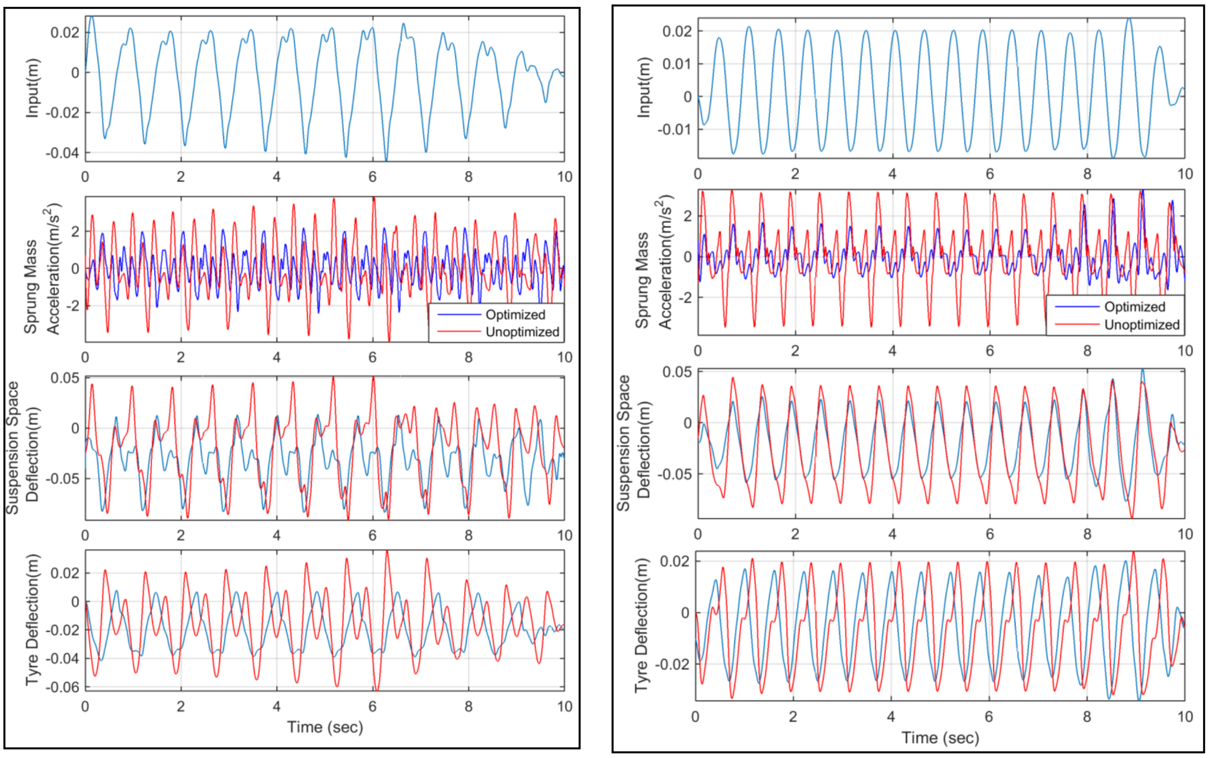

(**a**) (**b**)

Figure 14. Experimental Results – Time Domain: (**a**) Scenario-S4; (**b**) Scenario-S5.

3.2. Experimental Results – Actual Car

The optimization results are further extended over an actual car. For this study, a TATA Nano car is selected with Macpherson strut as a variable. The strut is already having setting of spring stiffness and damper for initial and optimum parameters.

Initially, a strut with original settings, i.e., un-optimized setting, is installed and is tested using 4 different drivers on 4 different road conditions. Table 8 and Table 9 represent driver data and road conditions, respectively. Road Case I-III are selected on Ahmednagar bypass highway, refer Figure 15 for Google Maps details. Here, for first two cases, speed of the vehicle is 40 and 60 kmph respectively, whereas Case-III a speed breaker is selected having 3 consecutive speed humps of height 25 cm and base of 30 cm. Case IV consists of a country road having considerable pot-holes and speed 20 kmph. Refer to Figure 16.

Table 8. Driver Data

Sr. No	Age (years)	Weight (kg)	Height (m)
Driver A	38	69	1.8034
Driver B	44	63	1.6891
Driver C	42	74	1.7880
Driver D	25	61	1.7272

Table 9. Road Details

Road Case	GPS Co-Ordinates	Test Condition
Road Case – I	(19.096890, 74.698216)	Speed 40 kmph.
Road Case – II	(19.096890, 74.698216)	Speed 60 kmph.
Road Case – III	(19.096890, 74.698216)	Speed breaker, 20 kmph.
Road Case – IV	(19.096011, 74.719690)	Country road, 20 kmph.

Figure 15. Ahmednagar Bypass Highway (Road Case – I-III). (Represented by Rectangle)

Figure 16. Country Road (Road Case – IV). (Represented by Arrows)

Then, strut with optimized settings is installed and tested with the same road conditions and drivers. Figure 17 and Figure 18 shows un-optimized and optimized results. The first row represents results of Road Case-I, the second row represent results of Road Case-II, the third row represent results of Road Case-III and fourth row represent results of Road Case-IV.

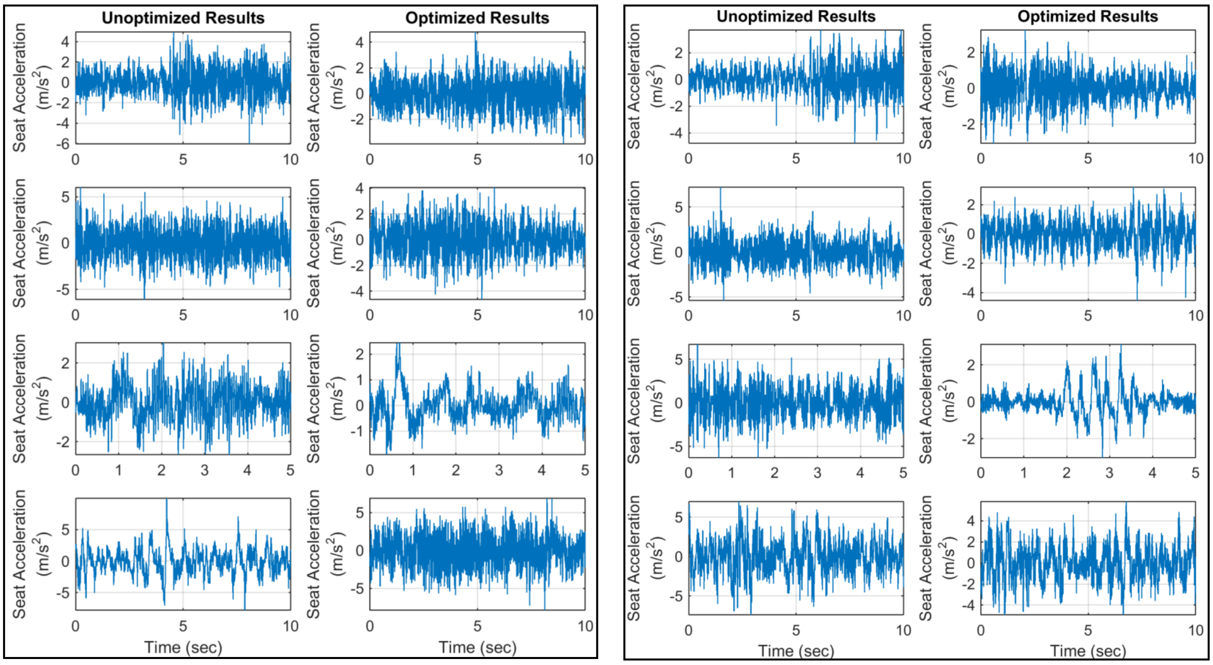

(**a**) (**b**)

Figure 17. Vehicle Results: (**a**) Driver A; (**b**) Driver B.

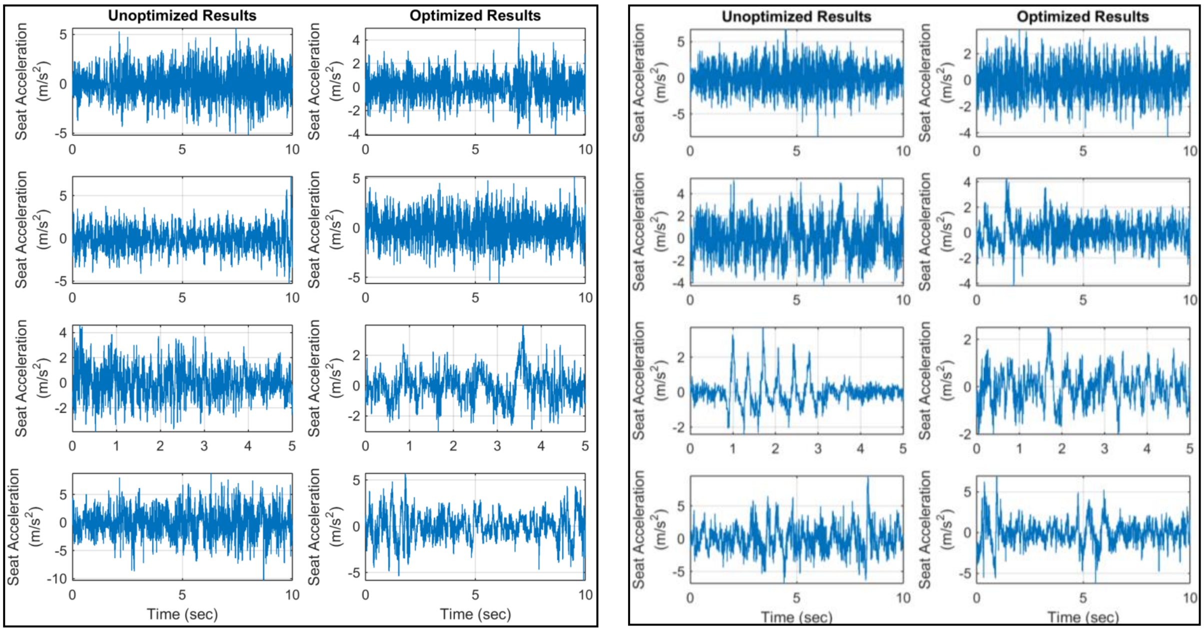

(**a**) (**b**)

Figure 18. Vehicle Results: (**a**) Driver C; (**b**) Driver D.

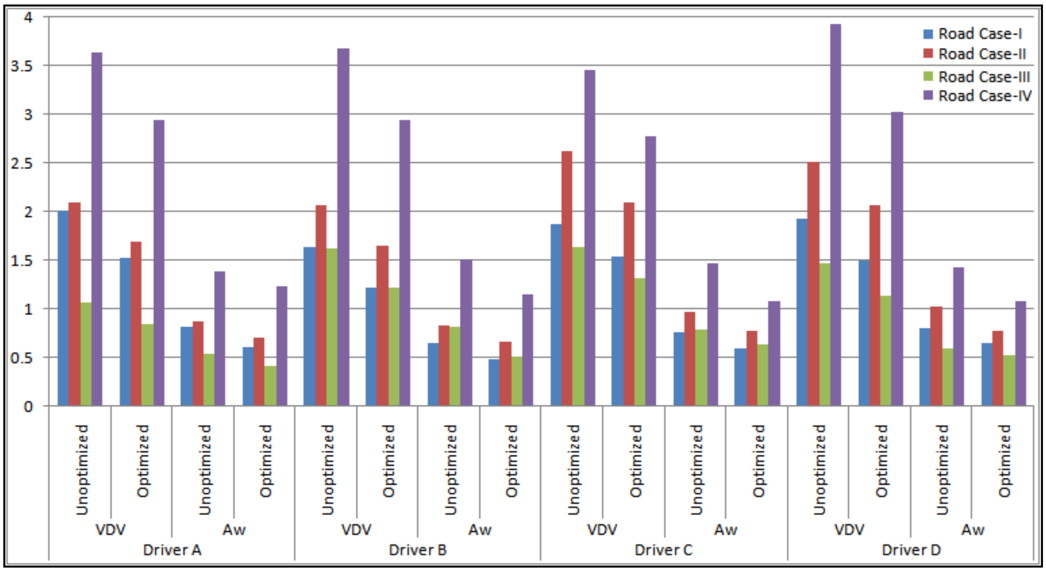

Figure 19. Bar Chart of Vehicle results – Optimized and Un-optimized system.

Table 10. VDV and Aw Values – Car Results.

Road Type	Un-optimized		Optimized		% Improvement	
	VDV	**Aw**	**VDV**	**Aw**	**VDV**	**Aw**
			Driver A			
Case-I	2.0164	0.8133	1.5306	0.6131	24.0958	24.6120
Case-II	2.1016	0.8725	1.7011	0.7128	19.0551	18.3018
Case-III	1.0674	0.5429	0.8461	0.4157	20.7319	23.4280
Case-IV	3.6347	1.3823	2.9461	1.2309	18.9454	10.9570
			Driver B			
Case-I	1.6440	0.6465	1.2286	0.4835	25.2676	25.2179
Case-II	2.0748	0.8267	1.6471	0.6603	20.6154	20.1204
Case-III	1.6202	0.8205	1.2228	0.5205	24.5309	36.5614
Case-IV	3.6844	1.5197	2.9387	1.1557	20.2399	23.9470
			Driver C			
Case-I	1.8730	0.7598	1.5473	0.5912	17.3849	22.1948
Case-II	2.6207	0.9665	2.0976	0.7822	19.9539	19.0717
Case-III	1.6391	0.7960	1.3172	0.6329	19.6414	20.4967
Case-IV	3.4579	1.4719	2.7770	1.0902	19.6906	25.9306
			Driver D			
Case-I	1.9283	0.8120	1.4992	0.6464	22.2527	20.3951
Case-II	2.5093	1.0316	2.0725	0.7804	17.4082	24.3553
Case-III	1.4764	0.5980	1.1338	0.5244	23.2077	12.3022
Case-IV	3.9299	1.4348	3.0241	1.0833	23.0491	24.4966

The VDV and Aw values are tabulated in Table 10. VDV and Aw are lowered by an average of 20% for optimized suspension systems compared to un-optimized ones. Figure 19 shows a bar chart that depicts both optimized and unoptimized results.

4. Conclusions

In this paper a Macpherson strut suspension system is modelled and simulated in MATLAB/Simulink® environment for ride comfort and optimization study.
The NSGA-II technique is used to define and optimize a multi-objective optimization of a Macpherson strut quarter vehicle. The optimization study includes objective functions such as comfort and health criteria involving RMS sprung mass acceleration, VDV, and MTTV, as well as stability criteria such as suspension and tire deflection.
A quarter car test setup is developed with Macpherson strut suspension system for experimental validation of optimization results. Simulated and experimental shows good correlation. It is observed that optimized parameters improve ride comfort and health criterions, and stability as compared to un-optimized system.
Among 5 scenarios of test results, maximum reduction of 47.80% in VDV is observed, a maximum of 47.66% reduction in RMS acceleration, 42.08% reduction in MTVV is observed. Frequency domain plot are used to present results. It is observed that optimum parameters are having improved results as comparted to initial or unoptimized suspension parameters.
Further, optimization parameters are implemented in an actual car. VDV and frequency weighted RMS acceleration are the two parameters under considerations for car results. Maximum improvement of 24.53% in VDV and maximum improvement of 36.56% in RMS acceleration is observed for the optimized suspension system. Thus, optimized suspension system not only improves ride quality but also improves health criterions.

Nomenclature

Aw	frequency weighted RMS accelration (m/s^2)
c_s	damping coefficient (N s/m) = 461
f	objective function
k_s	stiffness (N/m) = 15351 (Initial/Unoptimized value)
k_t	stiffness of tire (N/m) = 101134
l_A	distance between O and A (m) = 0.70
l_B	distance between O and B (m) = 0.35
l_C	control arm length (m) = 0.40
m_s	Sprung mass (kg) = 72.21
m_{us}	unpsrung mass (kg) = 23.56
VDV	vibration dose value (m/s$^{1.75}$)
v	velocity (m/s)
x_r	road profile (m)
x	displacement (m)
$\dot{x}$	velocity (m/s)
$\ddot{x}$	acceleration (m/s^2)
α	angle between link OA and horizontal (in ^{o}) = 60
Θ	control arm rotation angle (in ^{o})
Θ_o	initial angular displacement of control arm (in ^{o}) = -5

Subscripts (unless and otherwise stated)

s sprung

us unsprung

References

1. Alkhatib R, Jazar GN, Golnaraghi MF (2004) Optimal design of passive linear suspension using genetic algorithm. J Sound Vib. 275: 665–6591. https://doi.org/10.1016/j.jsv.2003.07.007.
2. Guo P, Zhang J-H (2017) Numerical model and multi-objective optimization analysis of vehicle vibration. J Zhejiang Univ Sci A. 18: 393–412. https://doi.org/10.1631/jzus.A1600124.
3. Nariman-Zadeh N, Salehpour M, Jamali A, Haghgoo E(2010) Pareto optimization of a five-degree of freedom vehicle vibration model using a multi-objective uniform-diversity genetic algorithm (MUGA). Eng Appl Artif Intell. 23: 543–551. https://doi.org/10.1016/j.engappai.2009.08.008.
4. Shojaeefard MH, Khalkhali A, Faghihian H, Dahmardeh M (2018) Optimal platform design using non-dominated sorting genetic algorithm II and technique for order of preference by similarity to ideal solution; application to automotive suspension system. Eng Optim. 50: 471–482. https://doi.org/10.1080/0305215X.2017.1324853.
5. Özcan D, Sönmez Ü, Güvenc L (2013) Optimisation of the Nonlinear Suspension Characteristics of a Light Commercial Vehicle. Int J Veh Technol. 2013: 1-16. https://doi.org/10.1155/2013/562424.
6. Chi Z, He Y, Naterer G (2008) Design Optimization of Vehicle Suspensions With A Quarter-Vehicle Model. Trans of the CSME /de La SCGM. 32: 297–312.
7. Kuznetsov A, Mammadov M, Sultan I, Hajilarov E (2011) Optimization of a quarter-car suspension model coupled with the driver biomechanical effects. J Sound Vib. 330: 2937–2946. https://doi.org/10.1016/j.jsv.2010.12.027.
8. Gündoğdu Ö (2007) Optimal seat and suspension design for a quarter car with driver model using genetic algorithms. Int J Ind Ergon. 37: 327–332. https://doi.org/10.1016/j.ergon.2006.11.005.
9. Patil SA, Joshi SG (2014) Experimental analysis of 2 DOF quarter-car passive and hydraulic active suspension systems for ride comfort. Syst Sci Control Eng. 2: 621–631. https://doi.org/10.1080/21642583.2014.913212.
10. Salah M (2017) A laboratory automotive suspension test rig: Design, implementation and integration. Jordan J Mech Ind Eng. 11: 67–71.
11. Koch G, Pellegrini E, Spirk S, Lohmann B (2010) Design and modeling of a quarter-vehicle test rig for active suspension control. Tech Univ München. 5: 1–28.
12. Ahmadian M, Pare C (2000) A quarter-car experimental analysis of alternative semiactive control methods. J Intell Mater Syst Struct. 11: 604–612. https://doi.org/10.1106/MR3W-5D8W-0LPL-WGUQ.
13. Sandu C, Andersen ER, Southward S (2011) Multibody dynamics modelling and system identification of a quarter-car test rig with McPherson strut suspension, Veh Syst Dyn. 49: 153-179. https://doi.org/10.1080/00423110903406664.
14. Hong K-S, Jeon D-S, Yoo W-S, Sunwoo H, Shin S-Y, Kim C-M, Park B-S (1999) A New Model and an Optimal Pole-Placement Control of the Macpherson Suspension System. SAE Tech Pap 1999-01-1331. 1999. https://doi.org/10.4271/1999-01-1331.
15. ISO: 2631-1. Mechanical vibration and shock – evaluation of human exposure to whole-body vibration (1997).
16. Van Niekerk JL, Pielemeier WJ, Greenberg JA (2003) The use of seat effective amplitude transmissibility (SEAT) values to predict dynamic seat comfort. J Sound Vib. 260: 867–888. https://doi.org/10.1016/S0022-460X(02)00934-3.
17. Bovenzi M (2005) Health effects of mechanical vibration. G Ital Med Lav Erg. 27(1): 58-64.
18. Baumal AE, Mcphee JJ, Calamai PH (1998) Application of genetic algorithms to the design optimization active vehicle suspension system. Comput Methods Appl Mech Eng. 163: 87–94. https://doi.org/10.1016/S0045-7825(98)00004-8.
19. Rosenthal S, Borschbach M (2014) Impact of Population Size and Selection within a Customized NSGA-II for Biochemical Optimization Assessed on the Basis of the Average Cuboid Volume Indicator. BIOTECHNO2014: 1–7.
20. Hernández-Díaz AG, Coello CAC, Pérez F, Caballero R, Molina J, Santana-Quintero LV (2008) Seeding the initial population of a multi-objective evolutionary algorithm using gradient-based information. 2008 IEEE Congr Evol Comput CEC 2008: 1617–1624 (2008). https://doi.org/10.1109/CEC.2008.4631008.
21. Reeves C, Rowe J (2003) Genetic algorithms – Principles and Perspectives A Guide to GA Theory, 1st ed., Dordrecht: Kluwer Academic Publisher.
22. Alander J (1992) On optimal population size of genetic algorithms 1992; Proceeding of CompEuro'92 'computer systems and software engineering. 65-70. https://doi.org/10.1109/CMPEUR.1992.218485
23. Deb K, Pratap A, Agarwal S, Meyarivan T (2002) A fast and elitist multiobjective genetic algorithm: NSGA-II. IEEE Trans Evol Comput. 6: 182–197. https://doi.org/10.1109/4235.996017.

24. Song L (2011) NGPM-A NSGA-II program in MATLAB – User Manual. Version 4 (1): 1-20.
25. Song L. NGPM-A NSGA-II Program in MATLAB V14. https://in.mathworks.com/matlabcentral/fileexchange/31166-ngpm-a-nsga-ii-program-in-matlab-v1-4(2021). Accessed 15 March 2021.